

## RESEARCH ARTICLE

10.1002/2017JD027339

## Key Points:

- The relative influence of a variety of environmental properties on sea breeze dynamics and aerosol transport is assessed and quantified
- Soil saturation fraction is an important factor for sea breeze properties and aerosol redistribution but is poorly represented in models
- The results provide guidance for future improvements in numerical weather prediction

## Correspondence to:

A. L. Igel,  
aigel@ucdavis.edu

## Citation:

Igel, A. L., van den Heever, S. C., & Johnson, J. S. (2018). Meteorological and land surface properties impacting sea breeze extent and aerosol distribution in a dry environment. *Journal of Geophysical Research: Atmospheres*, 123, 22–37. <https://doi.org/10.1002/2017JD027339>

Received 22 JUN 2017

Accepted 2 DEC 2017

Accepted article online 12 DEC 2017

Published online 4 JAN 2018

## Meteorological and Land Surface Properties Impacting Sea Breeze Extent and Aerosol Distribution in a Dry Environment

Adele L. Igel<sup>1,2</sup> , Susan C. van den Heever<sup>1</sup> , and Jill S. Johnson<sup>3</sup>

<sup>1</sup>Department of Atmospheric Science, Colorado State University, Fort Collins, CO, USA, <sup>2</sup>Department of Land, Air and Water Resources, University of California, Davis, CA, USA, <sup>3</sup>Institute for Climate and Atmospheric Science, University of Leeds, Leeds, UK

**Abstract** The properties of sea breeze circulations are influenced by a variety of meteorological and geophysical factors that interact with one another. These circulations can redistribute aerosol particles and pollution and therefore can play an important role in local air quality, as well as impact remote sensing. In this study, we select 11 factors that have the potential to impact either the sea breeze circulation properties and/or the spatial distribution of aerosols. Simulations are run to identify which of the 11 factors have the largest influence on the sea breeze properties and aerosol concentrations and to subsequently understand the mean response of these variables to the selected factors. All simulations are designed to be representative of conditions in coastal sub tropical environments and are thus relatively dry, as such they do not support deep convection associated with the sea breeze front. For this dry sea breeze regime, we find that the background wind speed was the most influential factor for the sea breeze propagation, with the soil saturation fraction also being important. For the spatial aerosol distribution, the most important factors were the soil moisture, sea-air temperature difference, and the initial boundary layer height. The importance of these factors seems to be strongly tied to the development of the surface-based mixed layer both ahead of and behind the sea breeze front. This study highlights potential avenues for further research regarding sea breeze dynamics and the impact of sea breeze circulations on pollution dispersion and remote sensing algorithms.

### 1. Introduction

Sea breeze circulations are ubiquitous along coastlines in the tropics and midlatitudes (Miller et al., 2003). From a basic physical standpoint, the mechanisms that govern their generation and maintenance are fairly well understood. Sea breezes are driven by differential daytime heating of the air over land and water surfaces. In the lower atmosphere, the relatively warm air over land is associated with locally low pressure, and likewise, the relatively cool air over ocean is associated with locally high pressure. This pressure gradient induces a baroclinic circulation with an inland-directed surface density current, a return flow aloft, and upward motions over land that can lead to the formation of clouds and precipitation if the environmental conditions are appropriate. Reviews of sea breeze dynamics are provided by Miller et al. (2003) and Crosman and Horel (2010).

Sea breezes have generated much interest for their ability to disperse pollutants that are emitted over land and, as such, can be an important control on air quality (e.g., Crosman & Horel, 2010) and remote sensing. In their review of pollutant outflow from southern Asia, Lawrence and Lelieveld (2010) argue that sea breeze circulations could be quite important for lofting pollution from the surface to higher elevations where it can be transported offshore. Once lofted, pollution plumes can bifurcate, and even be recirculated back into the onshore inflow layer (Lyons et al., 1995). Both studies conclude that a better understanding of the relationship between pollution dispersion and sea breezes is necessary. To further complicate the issue, other circulations such as trade winds, monsoon winds, and mountain flows may occur simultaneously with the sea breeze (Verma et al., 2006; Wang et al., 2013; Wang & Kirshbaum, 2017) to impact pollutant transport, and the spatial distribution of aerosols associated with sea breeze fronts can be heterogeneous. For example, enhanced optical depths have been observed with the passage of sea breeze fronts in both tropical (Moorthy et al., 1993) and desert (Derimian et al., 2017) settings. For these reasons, understanding the interactions between pollution and sea breezes is an active area of current research (Loughner et al., 2014; Mazzuca et al., 2017; Miao et al., 2015; Monteiro et al., 2016; Russo et al., 2016).

The redistribution of aerosols by coastal circulations is also of interest for remote sensing applications. Retrievals of quantities such as aerosol optical depth are particularly difficult in coastal zones due to sudden spatial and even temporal changes to land/ocean surface properties (Anderson et al., 2013) and due to uncertainties in the vertical distribution of aerosol particles. Better understanding of aerosol distribution in coastal zones could lead to improved retrievals and also to improved methods of assimilating these retrievals into numerical weather prediction models.

Despite our basic understanding of sea breeze circulations, it can be difficult to generalize the findings of single observational studies in order to understand which conditions have the most control on sea breeze characteristics and pollution dispersal. Generalizing previous studies is particularly challenging given that properties of the land surface and atmospheric conditions can interact to impact sea breeze characteristics in nonlinear ways (Baker et al., 2001; Grant & van den Heever, 2014). For example, Grant and van den Heever (2014) found that interactions between the effects of soil moisture and aerosol concentrations can lead to enhancements in precipitation greater than could be obtained by changing just one of these factors alone.

This study is designed to determine which atmosphere and land surface properties have the largest impact on sea breeze characteristics and associated aerosol transport within coastal zones through the use of idealized model simulations in order to better understand the general behavior of sea breezes. We investigate the mean response of the sea breeze to the most important properties and subsequently identify which properties most warrant further investigation. Since sea breezes have been found to impact aerosol and pollution transport in both humid and arid environments, we choose to begin with the relatively simple desert environment. Specifically, we examine the case of a relatively dry environment that does not support deep convection in order to keep the sea breeze dynamics relatively simple. Subsequent studies are currently investigating the case of a moist environment that does support deep convection and will address in detail how these properties impact the sea breeze and aerosol transport. This research is part of a larger, Multidisciplinary University Research Initiative (MURI) funded by the Office of Naval Research (ONR). The overarching goal of this project is to further our understanding and forecasting abilities of aerosol properties in coastal zones by bringing together expertise in satellite remote sensing, data assimilation, and high-resolution modeling to address fundamental questions about the controls on the spatial distribution and properties of aerosols in these areas.

## 2. Methodology

### 2.1. Overview

To address the goals of our study, we make use of a combination of idealized model simulations and statistical methods. Specifically, we make use of the methodological framework described in two recent studies that evaluated the effects of parametric uncertainty on simulated outputs from complex atmospheric models (Johnson et al., 2015; Lee et al., 2013). The approach begins with the identification of model parameters or initial conditions (factors) of interest and the assignment of an uncertainty range to each one in order to form a multidimensional parameter uncertainty space over which the model is explored. A perturbed parameter ensemble of model runs that optimally covers this parameter uncertainty space is then generated and used to construct Bayesian statistical emulators of different model output responses. Once validated, each emulator of a given model output can be used to densely sample that model output response across the full multidimensional uncertainty at a very low computational cost, enabling us to explore the model output behavior over the uncertainty and to identify (and quantify) key uncertainty sources.

In this study, we apply this framework to identify how changes in environmental characteristics impact on the sea breeze characteristics and aerosol transport and determine the environmental characteristics that are most influential. Our perturbed parameter ensemble consists of idealized model simulations that are loosely based on dry coastal environments. The simulations differ only in their initial conditions. They are not meant to exactly reproduce the conditions at any one time of year or location, but rather to capture representative conditions of these dry coastal regions. The strength of idealized simulations is that the physical insights and qualitative results gained from them are broadly applicable to many specific scenarios, even if the simulations did not account for the exact evolution of every geophysical variable in the specific situations.

We identify 11 factors (environmental characteristics) that we wish to test and use to vary the initial conditions in the ensemble. To select just three values for each factor and to run every combination for all 11 factors would require over 500,000 simulations. Since the model is computationally expensive, such a task is not feasible. By using a perturbed parameter ensemble consisting of only 143 simulations combined with the model output emulation, we can effectively run thousands of “virtual” simulations in a matter of minutes. This combination of modeling and statistical techniques therefore is a powerful and effective way to assess the relative importance of a large number of factors with a limited number of actual simulations. The use of idealized simulations further strengthens the utility of this method by making the results broadly applicable to many specific locations. In the following subsections, we will describe the basic model setup, the factors that have been chosen for investigation, how we vary these factors in the model initialization, and the statistical methods used for the analysis of the resulting simulations.

## 2.2. Basic Simulation Setup

The model used is the Regional Atmospheric Modeling System (RAMS) (Cotton et al., 2003; Saleeby & van den Heever, 2013). RAMS is a nonhydrostatic, fully compressible, atmospheric numerical model that has been successfully used in previous sea breeze modeling studies (e.g., Freitas et al., 2006; Grant & van den Heever, 2014). A grid spacing of 500 m in the horizontal was used. In the vertical, variable grid spacing was used that was 25 m between the lowest levels and stretched to 500 m after which the spacing was kept constant. There were a total of 57 vertical grid levels, with 17 of them within the first 1.5 km above the surface. Thus, the boundary layer processes were well resolved. Model integration employed a 5 s time step for 24 h, starting at 0000LT (local time). This allowed a land breeze to develop before dawn and a sea breeze to develop during the day.

Half of the domain used a land surface, and half used an ocean surface. The LEAF-3 (Walko et al., 2000) land surface model was used, and the land surface temperature and soil moisture are prognostic variables in this scheme. We used a desert surface type with sandy soil, representative of dry subtropical environments. Finally, the sea surface temperature was kept constant throughout the simulations and was varied with distance from the coast.

To achieve the goal of modeling sea breezes that are mostly free of moist convection, we based the initial conditions on dry subtropical coastal environments. The initial potential temperature and relative humidity profiles are created from ERA-Interim data for July 2014. This month was chosen since it corresponds to mid-summer when sea breezes in subtropical environments are frequent and long-lived (Azorin-Molina et al., 2011; Papanastasiou & Melas, 2009). The data were averaged along the North African coast between 20E and 30E (a somewhat arbitrary choice) on days with cloud fraction less than 0.01. The wind speed was initialized to be constant with height, and the wind direction was in the cross-coast direction. All atmospheric conditions were initially horizontally homogeneous. Gradients in temperature, pressure, moisture, etc. that typically form and drive sea breeze circulations quickly developed after the simulation start due to differing latent and sensible heat fluxes over land and ocean.

The Harrington (1997) radiation parameterization was used in all simulations. The day of year selected for these idealized tests was July 15. The aerosol parameterization is described by Saleeby and van den Heever (2013) and includes dry and wet deposition, depletion by cloud droplet nucleation, and regeneration upon droplet evaporation. The initial aerosol profile was horizontally homogeneous and decreased exponentially with height, with a maximum concentration of  $200 \text{ mg}^{-1}$  at the surface. We also initialized all simulations with a passive tracer field that was identical to the initial aerosol distribution. This tracer was transported by the wind but otherwise was not subject to any of the physical processes that the aerosol field experienced. Since most of the simulations analyzed here contained no clouds by design, the tracer closely mimics the behavior and evolution of the aerosol field and is also more representative of pollution that does not serve as cloud condensation nuclei (CCN).

## 2.3. Factors

Eleven model factors (parameters) that represent different environmental characteristics were selected for evaluation within this study. The chosen factors are listed with a short description in Table 1. The sea-air temperature difference ( $SST-T_a$ ), sea surface temperature gradient, land-air temperature difference ( $T_L-T_a$ ), and soil moisture content were chosen as these characteristics have the potential to impact surface sensible

**Table 1**  
 A List of the Factors Used in This Study, the Ranges Selected, and Their Descriptions

Factor	Range	Description
<i>Atmosphere factors</i>		
Stable layer strength	1 to 15 K km <sup>-1</sup>	Potential temperature lapse rate of the air layer immediately above the boundary layer
Stable layer depth	100 to 1,000 m	Depth of the air layer immediately above the boundary layer
BL potential temperature	285 to 300 K	Constant with height in the boundary layer
BL relative humidity	20 to 50%	Constant with height in the boundary layer. We recognize that a well-mixed boundary layer does not have constant relative humidity with height; however, this method ensured that we never accidentally began a simulation with supersaturated conditions. The boundary layer mixing quickly set up a realistic moisture profile after the simulations started.
BL height	100 to 1,000 m	Distance from the surface to the boundary layer top
Wind speed	-5 to 5 m s <sup>-1</sup>	Winds were perpendicular to the coastline. Both the speed and direction were constant with height throughout the depth of the troposphere. Wind shear has also been shown to impact sea breeze circulations (Drobinski et al., 2011) but was not tested here.
<i>Geophysical factors</i>		
SST- $T_a$	-10 to 10 K	Sea surface temperature (SST) minus the lowest level air temperature ( $T_a$ ). The factor ranges were chosen such that the SST was never below freezing.
SST gradient	-0.02 to 0.02 K km <sup>-1</sup>	The gradient was applied beginning at the coast such that the SST obtained from the SST- $T_a$ difference was valid at the coast. The ranges for both SST factors are based on the Reynolds SST analysis (Reynolds et al., 2007).
$T_f-T_a$	0 to 10 K	Land surface temperature ( $T_f$ ) minus the lowest level air temperature.
Soil moisture	0.1 to 0.9	Specified as a soil saturation fraction
Coriolis	0° to 45°	The Coriolis force was turned on in all simulations and was varied by changing the specified latitude. However, the chosen latitude did not impact the solar zenith angle or the incoming shortwave radiation. See text for more details.

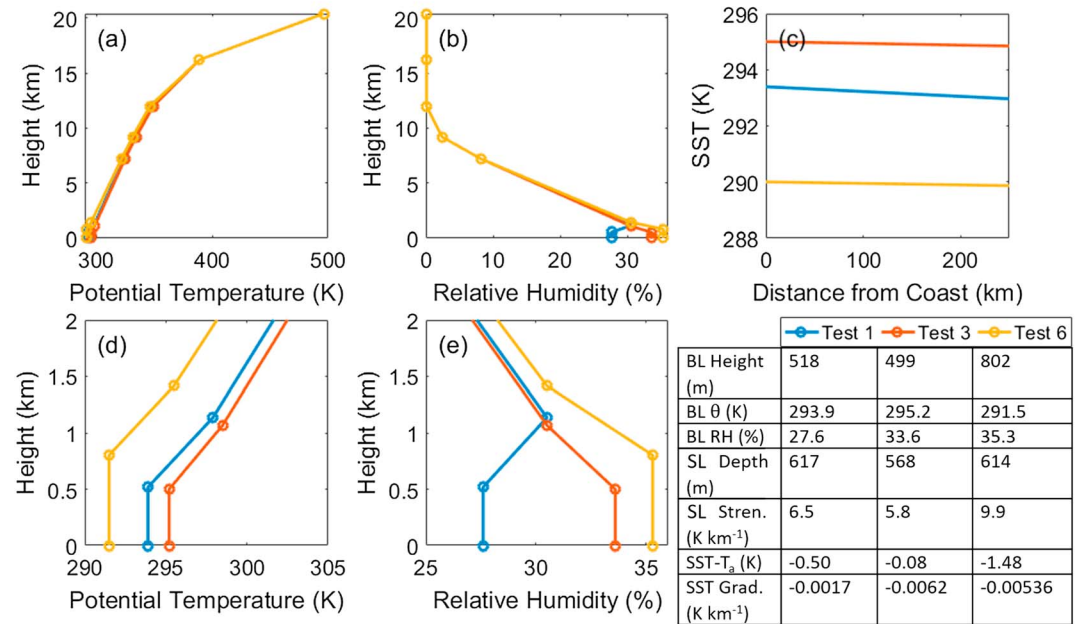
heat fluxes. The stable layer characteristics, boundary layer height, cross-coast wind speed, and Coriolis force (latitude) were chosen based on the review of sea breeze modeling studies (Crosman & Horel, 2010), which found these or related properties to be important for sea breeze dynamics. Finally, the remaining factors shown in Table 1 (boundary layer potential temperature and relative humidity) were included since they may have important implications for aerosol transport and cloud development. While clouds do not form frequently in the current study, we include these factors here for consistency with our follow-up study of moist sea breeze environments.

Table 1 also lists the plausible uncertainty range that we have assigned to each factor. These selected ranges combine to produce an 11-dimensional parameter uncertainty space over which we explore the behavior of the sea breeze and aerosol transport in our model. The values of all factors are initial conditions for the simulations, and except where noted in Table 1, the values of these factors evolve during the simulations.

Of course, there are many other factors that we could have chosen, but which have been excluded. For example, the initial conditions are horizontally homogeneous in the atmosphere (see section 2.2). In reality, gradients in temperature, humidity, and wind almost always exist in coastal zones, and these gradients could have been included as factors. We excluded these in the interest of keeping the study simple and idealized. Likewise, topographical variations such as land elevation and coastline curvature were also purposely excluded from this study in order to keep the model setup simple, as it is the simplicity of our setup that makes the results fundamental to the nature of sea breezes. That said, topographical variations will certainly have an impact on the sea breeze circulation and aerosol transport (e.g., Baker et al., 2001) and will be addressed in separate studies.

#### 2.4. Use of the Factors to Initialize Simulations

The factors described in Table 1 are used to vary the initial conditions for the simulations. Following Lee et al. (2011) and Johnson et al. (2015), we use the maximin Latin hypercube design algorithm to produce an ensemble of 143 factor value combinations that provide an optimal coverage of our 11-dimensional parameter uncertainty space. We then use these 143 factor value combinations to initialize 143 RAMS simulations.



**Figure 1.** Example initial conditions from Tests 1, 3, and 6. (a) Potential temperature profiles, (b) relative humidity profiles, and (c) sea surface temperature as a function of distance from the coast. (d and e) Similar to Figures 1a and 1b, respectively, but show only the lowest 2 km of the atmosphere. The table shows the values of the relevant factors.

The application of wind speed, boundary layer, and stable layer characteristics as initial conditions is straightforward (see Table 1 for details). Positive wind speed values correspond to initially offshore flow, and negative values correspond to initially onshore flow. Above the stable layer, the relative humidity profiles were identical for all simulations. The potential temperature profiles all had the same dry static stability up to 200 mb. At 100 and 50 mb (in the stratosphere), the potential temperature is the same in all simulations. Example initial conditions for relative humidity and potential temperature from three simulations are shown in Figure 1.

The Coriolis force is varied by changing the latitude. Latitude, of course, also impacts the incoming solar radiation. Therefore, the latitude is set to 0°, the minimum value in our allowed range for the Coriolis force, for all radiation calculations in all simulations. Although this is not a subtropical latitude, it is consistent with the value used in our follow-up study for moist environments, as is the range of latitudes tested for the Coriolis force. Furthermore, the same total daily insolation can be found at the highest latitudes tested in late summer, and therefore, the insolation is not unrepresentative of these latitudes. That said, the choice of radiative latitude will have a large impact on the evolution of the sea breeze, but we do not expect that choosing a different radiative latitude would qualitatively alter the results of this study.

The use of the remaining factors as initial conditions to RAMS is fully described in Table 1.

### 2.5. Analysis

For each model output of interest (see Sections 3.3 and 4.2), we use our perturbed parameter ensemble of model runs to construct a statistical emulator (O’Hagan, 2006) of the output over the parameter uncertainty space. This emulator is constructed using the output of the first 121 simulations in our ensemble, using the statistical software R (R Core Team, 2015) and the R package DiceKriging (Roustant et al., 2012), and is validated with the remaining 22 simulations. Here the emulator model provides a mapping of the relationship between the 11-dimensional parameter uncertainty space and the corresponding model output that is fast to evaluate and can be used to predict the value of the output with uncertainty at any combination of the factor values.

Using these statistical emulators, we then apply variance-based sensitivity analysis techniques (Saltelli et al., 2000) to decompose and proportionally assign the variation in each model output to the factors. Here we

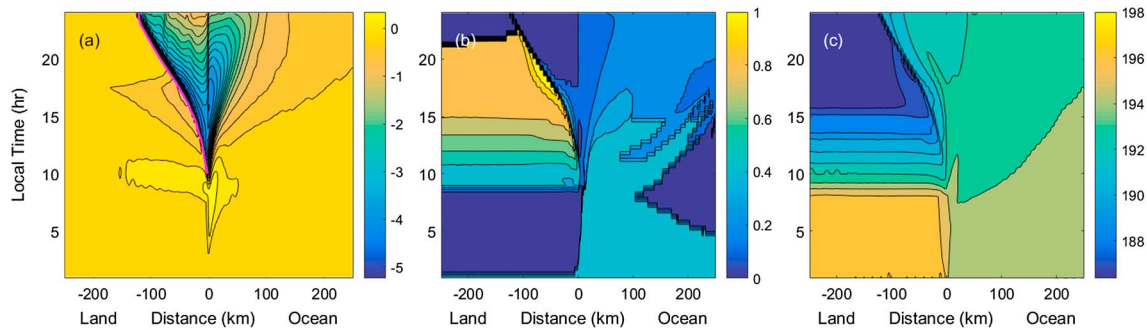


**Figure 2.** Example evolution of the sea breeze from Test 1. Shaded contours show (a) wind speed ( $\text{m s}^{-1}$ ) perpendicular to the coast, (b) surface-based mixed layer depth (km), and (c) tracer surface concentration ( $\text{mg kg}^{-1}$ ). The pink line shows the location of the objectively identified sea breeze.

apply the extended Fourier amplitude sensitivity test approach of Saltelli et al. (1999) to compute the sensitivity measures, using the R package “sensitivity” (Pujol et al., 2013) to perform the calculations. The reported percentage of variance attributed to each factor here is interpreted as the direct contribution of the factor to the overall variance in the given model output and does not include any contributions due to factor interactions.

### 3. Sea Breeze Characteristics

#### 3.1. Sea Breeze Identification

The sea breeze was objectively identified for all 143 simulations. The identification algorithm is described in Appendix A. An example of a simulated sea breeze from one of the model runs and the corresponding objectively identified sea breeze is shown in Figure 2a. In this case, the onset of the sea breeze is at 0900 LT, which is consistent with typical sea breeze onset times for the subtropical environments (Azorin-Molina et al., 2011; Papanastasiou & Melas, 2009). A weak land breeze had developed before sunrise. Overall, the algorithm performs very well in all cases (not shown). In addition, no sea breeze developed in 16 out of the 143 simulations in our ensemble. The algorithm correctly fails to identify a sea breeze in all of these simulations.

#### 3.2. Average Behavior

First, we look at the average behavior of the sea breeze in the simulations. Figure 3 shows the mean and standard deviation of the location of the sea breeze front and the average propagation speed as a function of time. All 143 simulations in our ensemble were used to create this figure. It can be seen that, on average, the sea breeze propagates almost 150 km inland in these idealized simulations that do not have topographical barriers. The standard deviation of the final extent is about 50 km, which indicates that there is a substantial amount of variability in the sea breeze evolution across the ensemble. The average propagation speed increases with time until about 1900 LT (1 h after sunset). The simulated idealized sea breeze acceleration is consistent with previous modeling results (e.g., Sha et al., 1991; Yan & Anthes, 1987) and observations (e.g., Physick & Smith, 1985; Simpson et al., 1977).

Since one of our objectives in this study is to better understand near-surface aerosol redistribution by sea breezes, we also examine the depth of the surface-based mixed layer. We identified this depth as the height from the surface at which the vertical potential temperature gradient first exceeds  $2 \text{ K km}^{-1}$ . Other threshold values were tried but did not qualitatively change the results. An example of the evolution of the mixed layer depth is shown in Figure 2b. It is clear that the mixed layer depth is strongly impacted by the sea breeze here. Ahead of the sea breeze front, where the boundary layer is primarily controlled by the direct daytime heating and surface fluxes, the mixed layer depth exceeds 1 km. Behind the sea breeze front, the mixed layer is quite shallow—in this case, less than 200 m.

The average surface-based mixed layer depth for all simulations averaged over land behind the sea breeze front (coast to the front) is shown in Figure 3c. It increases until midday, slowly decreases during the afternoon, and rapidly decreases after sunset.

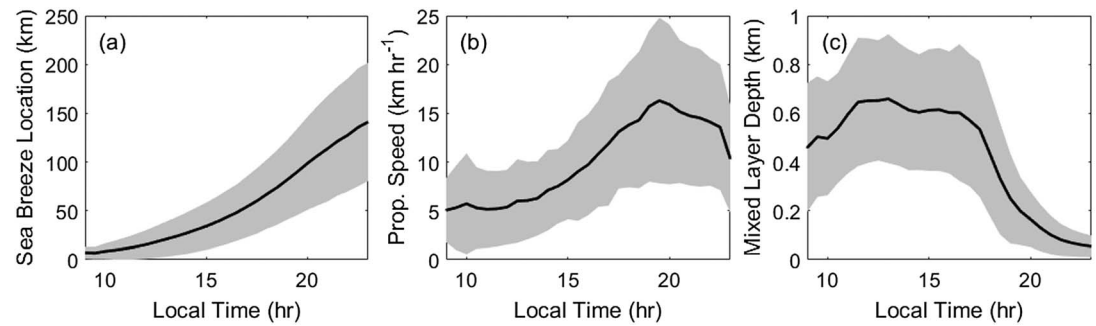


**Figure 3.** Mean and  $\pm 1$  standard deviation of the (a) location of the sea breeze front (km inland), (b) the propagation speed (m/s), and (c) the surface-based mixed layer depth behind the sea breeze front from all 143 simulations.

### 3.3. Sensitivity Analysis

To investigate the impact of the uncertainty in our eleven factors on the sea breeze, we have constructed a statistical emulator and applied the variance-based sensitivity analysis method for the following three characteristics of the sea breeze: the maximum extent, the difference in propagation speed during the night and day (a simple measure of the sea breeze acceleration), and the surface-based mixed layer depth behind the sea breeze front.

The daytime propagation speed was calculated as the position at 1800 LT (sunset) divided by the total time that the sea breeze had been in existence, whereas the nighttime propagation speed was calculated as the difference in the maximum position and the position at 1800 LT divided by the time in that interval. In a few cases the sea breeze exited the domain before the end of the simulation (e.g., Figure A1a). In these cases, the maximum extent was estimated by extrapolating the sea breeze position to 2400 LT using the nighttime propagation speed. Simulations that did not produce a sea breeze were assigned values of 0 for the maximum sea breeze extent and propagation speeds.

The mixed layer depth was taken as the maximum value in time of the average depth between the coast and the sea breeze front. Simulations without a sea breeze were assigned the maximum value in time of the average depth over all land.

The factor combinations that were used to generate each of the 22 reserved validation simulations were input to the statistical emulators of the three sea breeze characteristics to obtain the corresponding emulator mean predictions and 95% confidence bounds on these predictions in each case. These predicted values were compared to the actual simulated values from the RAMS simulations to ensure that the statistical emulators are robust. Figure 4 shows this information and demonstrates that the emulators for all three selected sea breeze characteristics provide good predictions. With the exception of three predictions (two for the sea breeze extent and one for the mixed layer depth), all other emulator predictions (63 in total, or 95%) agree with the RAMS modeled values within the 95% confidence bounds. These results give us confidence that the emulators are accurately representing the true response of each characteristic to the 11 factors under study.

To understand which factors contribute most to the variability of the sea breeze extent, the night-day propagation speed difference, and the mixed layer depth, we have used the variance-based sensitivity analysis approach of Saltelli et al. (1999) to calculate the percentage of output variance attributable to each factor. The results of this analysis are shown in Figure 5 and discussed in the following subsections.

#### 3.3.1. Maximum Extent

The initial wind speed is by far the most important factor in determining the maximum sea breeze extent and explains about 75% of the variance (blue bars in Figure 5). Figure 6a shows the mean response of the maximum extent to the wind speed, sea-air temperature difference, and soil saturation fraction, determined through simulation from the statistical emulator for this output. Over the range of each factor here, the value of the mean response for the maximum extent at a particular factor value (on the x axis) is calculated as the mean of 500 predictions (increasing the number of predictions minimally changes the mean) from the emulator that take the given value for this factor of interest and uniformly random values for all other factors.

In Figure 6a, onshore environmental winds (green line; negative values) cause the sea breeze to propagate further inland, and vice versa for offshore winds (positive values). This result regarding offshore flow is

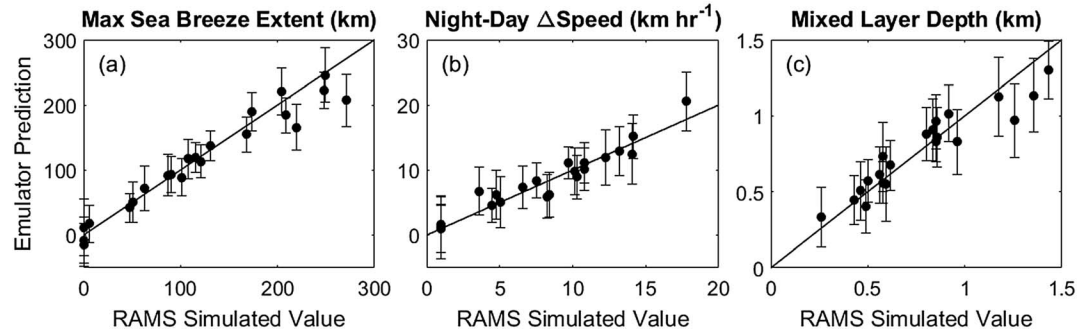


**Figure 4.** Validation of the emulator for (a) maximum sea breeze extent, (b) difference in nighttime and daytime propagation speed, and (c) surface-based mixed layer depth over land behind the sea breeze front. The x axis shows the values predicted by the RAMS simulations, and the y axis shows the values predicted by the emulator, with 95% confidence bounds. The solid line is the 1-to-1 line, which indicates where the emulator and RAMS predict the same value.

consistent with previous studies (e.g., Arritt, 1993; Finkle, 1998) that have found that strong offshore flow will reduce the inland penetration of the sea breeze. Also in agreement with our results, laboratory experiments with density currents show that an onshore flow would lead to faster propagation (Simpson & Britter, 1980). However, some studies suggest that sea breeze inland penetration should be retarded, not enhanced, by strong onshore flow due to a reduced temperature gradient between land and sea (Chiba et al., 1999; Simpson, 1994). Our simulations do show that sea breeze fronts with the strongest temperature gradients formed in initially light winds, but they still had only medium values of inland extent (Figure 7). In three of the 143 simulations, the sea breeze stops propagating before the end of the simulation, and in these three cases, the winds are initially onshore (not shown). However, in most cases, the onshore winds do not prevent the sea breeze from propagating a far distance inland despite reduced temperature gradients.

The next two most important factors contributing to the maximum extent of the sea breeze are the soil saturation fraction and the sea-air temperature difference, which explain about 13%, and 7% of the variance, respectively (blue bars in Figure 5). Warmer sea surface temperature relative to the air (blue line; values greater than 0 in Figure 6a) leads to slower moving sea breezes that do not extend as far inland. This is due to a reduced air temperature gradient between the land and ocean and is in line with our expectations and understanding of sea breeze circulation thermodynamics. Higher soil moisture also reduces the sea breeze extent (gray line in Figure 6a). Higher soil moisture reduces the sensible heat flux over land and, as with warmer sea surface temperatures, leads to a reduced gradient in air temperature between the land

and over the ocean. These two factors are approximately equally important on average.

**3.3.2. Sea Breeze Acceleration**

Figure 5 (teal bars) reveals that the initial wind speed is also the most important factor for setting the night-day propagation speed difference. However, for this sea breeze characteristic, the soil saturation fraction is of almost equal importance to the initial wind speed. As with the maximum sea breeze extent, stronger offshore flow and higher soil moisture lead to reduced sea breeze acceleration (green and dark gray lines in Figure 6b). We hypothesize that low soil moisture can promote rapid cooling of the land surface near and after sunset, thereby inducing a negative sensible heat flux. Winds are relatively calm ahead of the front and stronger behind (on the oceanward side). This leads to stronger cooling of the air behind the sea breeze front and enhances the temperature gradient across the front (not shown), which would increase the propagation speed of the front (Simpson & Britter, 1980).

The initial sea-air temperature difference and the Coriolis effect are of secondary importance for the sea breeze acceleration (teal bars in Figure 5). Relatively cold sea temperatures lead to greater acceleration of the sea breeze (blue line in Figure 6b), which is consistent with sea breezes that

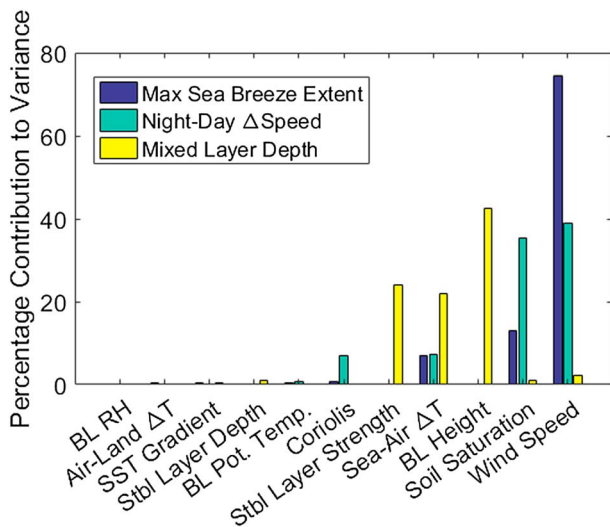


**Figure 5.** Percentage contribution to variance for the maximum sea breeze extent (navy bars), nighttime minus daytime propagation speed (teal bars), and mixed layer depth (yellow bars) by each of the eleven factors.



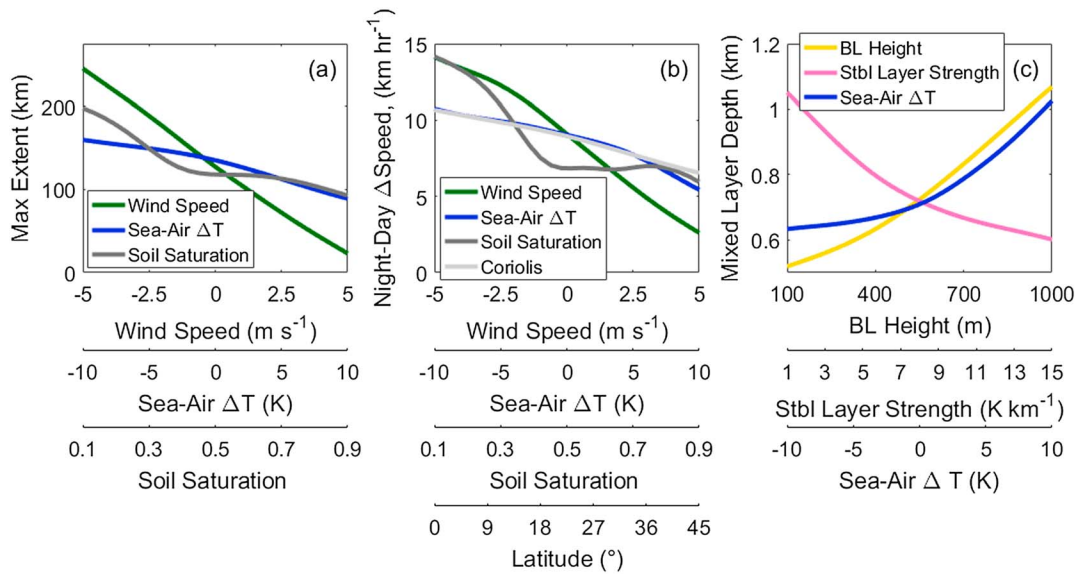


**Figure 6.** Mean response of the (a) maximum sea breeze extent (km), (b) nighttime minus daytime propagation speed, and (c) surface-based mixed layer depth behind the sea breeze front to the factors that contribute 5% or more to the output variance in each case. Each line corresponds to a different x axis.

penetrate further inland (blue line in Figure 6a). A stronger Coriolis effect limits the acceleration of the sea breeze (light gray line in Figure 6b) due to the turning of the winds by the Coriolis force (Rotunno, 1983; Yan & Anthes, 1987).

### 3.3.3. Mixed Layer Depth

Different factors are responsible for controlling the variation in the depth of the sea breeze mixed layer than for controlling the sea breeze maximum extent and acceleration. The initial boundary layer height and stable layer strength are the two most important factors for the mixed layer depth (yellow bars in Figure 5). Initially, deep boundary layers capped by weak stable layers promote deeper mixed layers between the sea breeze front and the coast (yellow and pink lines in Figure 6c). Relatively warm ocean temperatures also promote deeper mixed layers (blue line in Figure 6c). We note that despite the fact that these mixed layers exist over land, the sea surface temperature plays a bigger role in their depth than the land surface characteristics since this air mass is largely advected from over the ocean to over land. Ahead of the sea breeze front, the mixed layer depth is also strongly controlled by the soil saturation, but not the sea surface temperature (not shown).

The other factors do not contribute to a high percentage of the variance of the sea breeze characteristics that were analyzed here. This fact does not imply that these factors have no impact at all. Rather, the factors with a low contribution to variance have a relatively small impact *on average* compared to the other factors that were analyzed. The insignificant factors to the mean may be quite important in certain specific situations, but it is not the intention of this study to understand what those situations are. The intention of the study is to identify the factors that have the largest impacts on average and to understand the average response of the sea breeze characteristics to those factors.

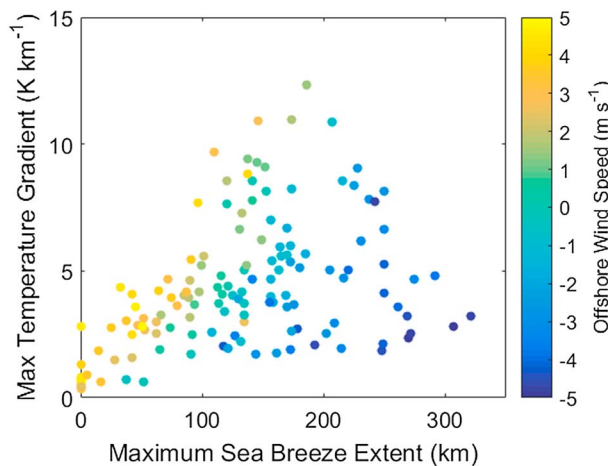


**Figure 7.** Scatter plot of the maximum sea breeze extent (km) and the time and domain maximum surface temperature gradient ( $K km^{-1}$ ). Points have been colored according to the initial cross-coast wind speed ( $m s^{-1}$ ). The positive values indicate offshore winds, and the negative values indicate onshore winds.

## 4. Aerosol Response

### 4.1. Overview

The impact of the eleven factors on the properties of the aerosol spatial distribution in the vicinity of the sea breeze front and coast was also investigated. Since a few simulations did produce clouds that reduced aerosol

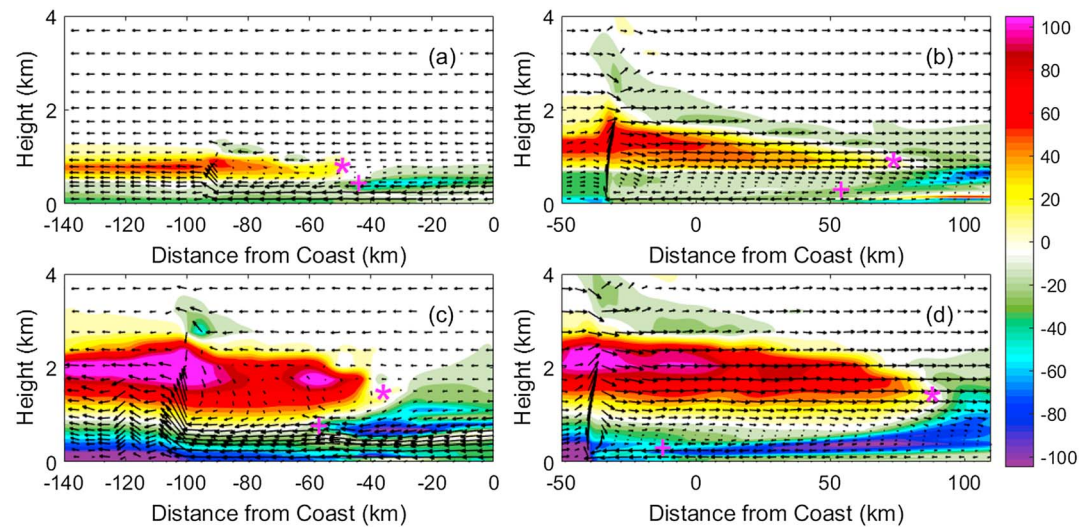


**Figure 8.** Examples from four simulations of the tracer perturbation field ( $\text{mg}^{-1}$ ) (1800 LT minus 0600 LT) and the cross-coast wind circulation. The simulations are chosen to demonstrate the impacts of the initial wind speed and soil moisture. Specifically, (a) low soil moisture and onshore wind, (b) low soil moisture and offshore wind, (c) moderate soil moisture and onshore wind, and (d) moderate soil moisture and offshore wind. The pink stars show the locations of the vented plume head, and the pink crosses show the locations of the clean plume head.

concentrations, we chose to analyze the tracer field as a proxy for the aerosol concentration, or other air pollutants that do not serve as CCN.

First, Figure 8 shows four examples of the sea breeze circulation at 1800 LT and the change in tracer concentration between 0600 (sunrise) and 1800 LT. Land is on the left of the figure, and ocean is on the right. These four examples were chosen to illustrate the impacts of wind speed and soil moisture on the simulations. The sea breeze front location is clearly identifiable in all cases as the place where there is a sudden upward component in the wind vectors. In the right-hand column of Figure 8, the sea breeze circulation has a clear inflow branch near the surface and a clear return flow above about 1 km. Both of these example simulations were initialized with offshore winds. In the left-hand column, simulations with initially onshore winds are shown, and it is seen that while the sea breeze penetration inland is much greater, the return flow is much weaker. Nonetheless, all four examples show similar structures in the tracer perturbation field. Ahead of the sea breeze front, positive perturbations overlay negative perturbations due to the daytime mixing of the boundary layer and the fact that the simulations were initialized with an exponentially decreasing profile of tracer concentration. As the sea breeze front impinges on this air, the positive perturbation plume is vented out of the boundary layer oceanward in the return flow of the sea breeze circulation. This structure is similar to that seen in sea breeze simulations by Lu and Turco (1994) and Verma et al. (2006). The edge or head of this vented air mass is clearly seen by the sharp horizontal gradient of aerosol perturbation marked by the pink stars in Figure 8. It is objectively identified as the most oceanward point with at least a  $10 \text{ mg}^{-1}$  tracer perturbation. In addition, some of these vented tracers may be advected further upwards by the vertical motions occurring right at the sea breeze front. However, since the convection at the sea breeze front is dry in these simulations, the vertical motions are not particularly strong, and most of this plume is advected horizontally.

On the oceanward side of the sea breeze front, tracer perturbations at and near the surface are almost universally negative. Further aloft, we also see widespread areas of negative aerosol perturbations. These maximize at or slightly below the level of the vented head and seem to be associated with slightly subsiding air that is originating over the ocean and may become incorporated in the sea breeze circulation inflow. The edge of this subsiding ocean air plume is marked with pink crosses in Figure 8 and will be called the “clean plume head.” It is objectively identified as the most landward point along the minimum closed negative perturbation contour (most landward point that is distinguishable from the negative perturbations due to boundary layer mixing). We now use the statistical framework described above to understand which factors most control and influence the properties of the spatial distribution

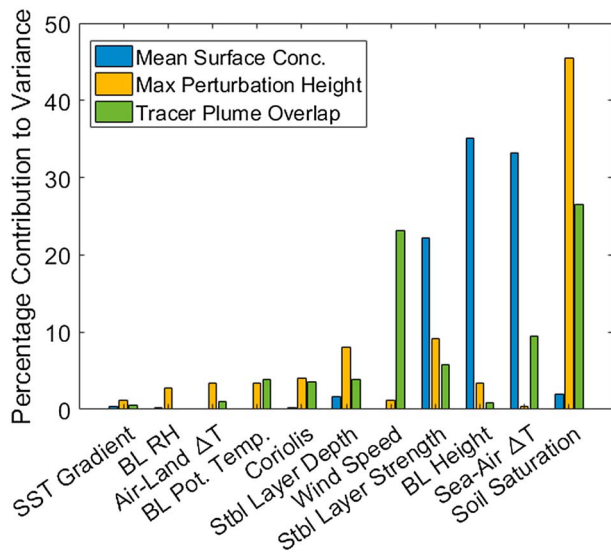


**Figure 9.** Like Figure 5, but for the mean surface tracer concentration between the coast and the sea breeze front at 1800 LT (blue bars), maximum height of a 1% positive perturbation in tracer concentration (orange bars), and the overlap distance of the clean and vented plumes (green bars). See the text for more details.

of the tracer. Specifically, we look at the mean surface concentration between the coast and the sea breeze front, the maximum height of a 1% positive aerosol perturbation, and the relative positions of the vented and clean plume heads. Each of these output properties is now discussed in more detail in the following subsections.

**4.2. Sensitivity Analysis**

**4.2.1. Average Surface Concentration**

The average surface concentration of the tracers between the coast and the sea breeze front was analyzed every 3 h starting at 1200 LT. As with the sea breeze characteristics, a statistical emulator of these model responses (one emulator at each time output) was constructed and validated (not shown), and variance-based sensitivity analysis was used to determine the percentage of variance in the tracer concentration attributable to each individual factor.

The blue bars in Figure 9 show the percentage of variance of the average surface tracer concentration explained by each of the 11 factors. Only the results for 1800 LT are shown; all other times showed qualitatively similar results. The initial boundary layer height, sea-air temperature difference, and initial stable layer strength all contribute 20% or more to the variance in the average surface concentration and combined explain 91% of the variance. Even at 2400 LT, these factors together explain 84% of the variance (not shown). These are the same three factors that contributed the

most variance to the maximum boundary layer height in Figure 5. Furthermore, the average response of the surface tracer concentration to each of these factors (Figure 10a) mirrors the average response of the boundary layer depth (Figure 6c), but the trends each have opposite signs. A scatterplot of the mean surface tracer concentration between the coast and the front at 1800 LT and the maximum boundary layer height for the same region confirms the close relationship (Figure 11). Namely, as would be expected, deep boundary layers lead to more mixing and a reduction of the surface tracer concentration. The color and size of the points in the figure indicate the sea-air temperature difference and initial stable layer height, respectively. Qualitatively, the pattern of color and size is consistent with the statistical results.

These results suggest that boundary layer mixing is the most important control on surface tracer concentration behind the sea breeze front. Transport of tracers from locations other than the marine boundary layer, such as the recirculation of vented tracers associated with the sea breeze circulation, is relatively minor in magnitude. The inland extent of a sea breeze and accompanying tracer concentrations will also be important in determining its impact on the local air quality. As such, factors that determine the sea breeze extent and speed such as the initial wind speed and soil saturation (Figure 5) will also be important for determining local tracer and aerosol concentrations.

**4.2.2. Maximum Perturbation Height**

The orange bars in Figure 9 indicate that only one factor contributes more than 10% to the variance of the maximum height of a 1% tracer perturbation, namely, soil saturation. It accounts for 45% of the variance. The stable layer depth and strength combined contribute another 17% of the variance, but each on its own contributes less than 10%. Moist soil leads to smaller perturbation heights (Figure 10b), but the effect becomes negligible at about 0.4 soil saturation fraction. We hypothesize that there are two reasons for the dominance of the soil saturation. Dry soil will promote sensible rather than latent heat fluxes and thus cause more heating of the near surface air. First, this additional heating helps to deepen the boundary layer ahead of the sea breeze front (not shown), the region which, as discussed above, is the main source of the positive tracer perturbations. Second, warmer near surface air that enters the frontal updraft will be more buoyant, rise to higher heights, and transport high tracer concentrations to those higher heights.

**4.2.3. Tracer Plume Overlap**

Finally, we analyze the relative positions of the clean and vented plume heads. This metric gives an indication of the extent to which the two plumes are interacting, or will interact and mix in the future. It also indicates, to

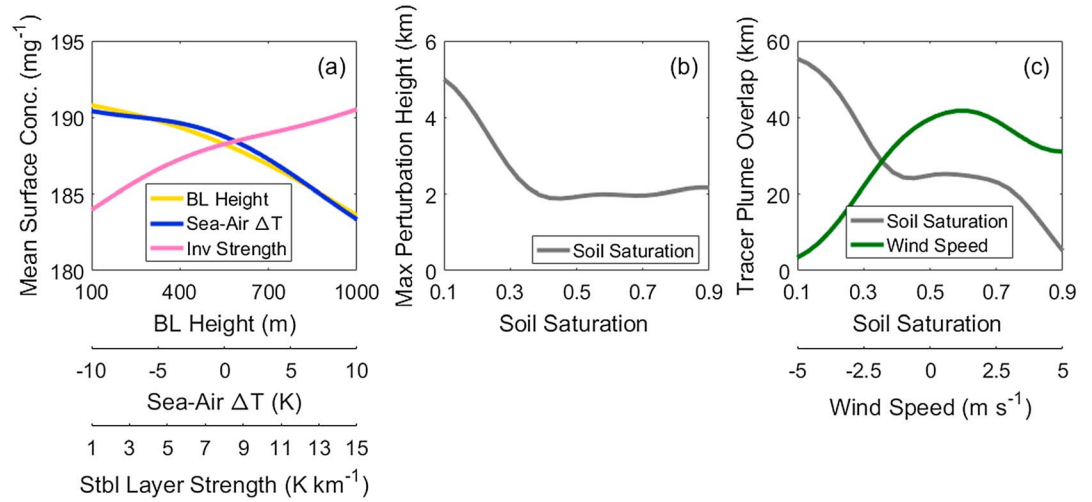


**Figure 10.** Like Figure 6, but showing the mean response of factors for each of the three aerosol tracer-related model outputs that contribute 10% or more to the model response.

some degree, the likelihood that the clean plume will mix/has mixed with the inflow air. The green bars in Figure 9 show that the wind speed and the soil saturation fraction contribute more or less equally to the variance of this output metric and combined explain about 50% of this variance. The other factors and/or interactions among the factors explain the other 50%. Moister soil leads to less overlap in the plumes, whereas neutral to weak offshore winds most favor large overlap (Figure 10c). The four example simulations in Figure 8 were intentionally chosen to demonstrate the importance of these two factors. As mentioned before, the left and right columns show simulations with initially onshore and offshore winds, respectively. In each column, the winds have approximately the same magnitude. Similarly, the top and bottom rows show simulations with similar moderate and low values of the soil saturation fraction, respectively. Of course, all of the other factors vary among these four simulations, and so will also contribute to differences in these sea breeze circulations and tracer perturbation fields. Nonetheless, they do demonstrate that low soil moisture tends to lead to deeper boundary layers ahead of the front and deeper, more pronounced vented plumes that allow the clean plumes to undercut them more easily. As for the wind factor, while all simulations have a well-defined inflow, only the simulations with background offshore flow can efficiently vent the tracers back toward the ocean and override clean plumes.

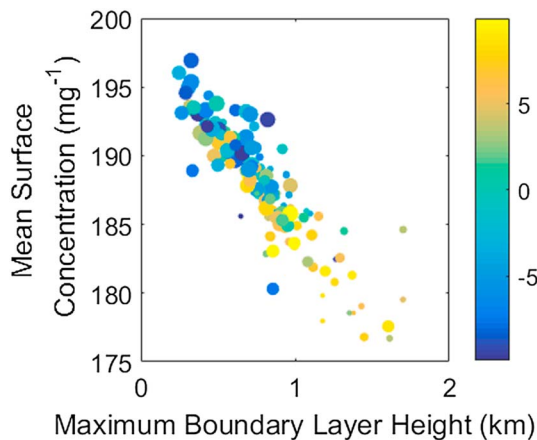


**Figure 11.** Scatterplot of the average surface tracer concentration at 1800 LT and maximum boundary layer height between the coast and the sea breeze front from all 143 simulations. The colors indicate the sea-air temperature difference (K), and the size indicates the initial stable layer strength. The large (small) sizes correspond to strong (weak) stable layers.

### 5. Conclusions

In this study, our goal was to identify the most important meteorological and geophysical factors that contribute to variability in sea breeze circulations and aerosol spatial distribution. Our results have applications and implications for numerical weather prediction, air quality, and remote sensing in coastal zones. Although previous studies have identified numerous factors that contribute to sea breeze and aerosol spatial distribution; this is the first study to do so in a way that evaluates numerous factors simultaneously using advanced statistical methods that allowed us to compare the relative importance of the factors. To do so, we ran a large perturbed parameter ensemble of simulations with a cloud-resolving model and interactive land-surface model. Of the factors tested, the initial wind speed had the largest impact on the maximum sea breeze extent, followed by the soil moisture content and the sea-air temperature difference. Onshore flow was not found to retard the sea breeze propagation

distance as has been suggested by some previous studies (Chiba et al., 1999; Simpson, 1994), but rather consistently led to sea breezes that propagated the furthest distances inland. The soil moisture content was especially important for controlling how much the sea breeze front accelerated between the day and night.

We also assessed the relative importance of the same factors for the redistribution of a tracer field that was representative of pollutant concentrations within the coastal zone. Behind the sea breeze front, the surface tracer concentrations were strongly linked to the same factors that controlled mixed-layer depth. This result demonstrates that over land behind the sea breeze front, ocean characteristics are more important than land characteristics for determining the degree of vertical mixing and that vented pollutants were not efficiently recirculated into the sea breeze inflow air. The maximum height of the vented pollutants was most influenced by the soil moisture. We also examined the degree to which the vented pollutants had the potential to mix with cleaner ocean air that was being drawn into the sea breeze inflow. Wind speed and again soil moisture were found to be the two most important factors for controlling this interaction.

When considering ways to improve numerical weather prediction, this study serves as a guide for potential avenues of improvement of sea breezes and aerosol redistribution forecasts. While large-scale winds are already well simulated in forecast models, better representation of sea surface temperatures, especially in coastal zones where coarse sea surface temperature analysis products may not appropriately capture local conditions (Lombardo et al., 2016), may lead to improvements in forecasts of aerosol redistribution. While the importance of sea surface temperature has long been recognized, this is the first study to show that it is one of the *leading* causes of uncertainty. Of the factors tested, soil moisture was found to be the most important overall for aerosol redistribution, yet it may also be the most uncertain in current models. It is frequently not well represented in models (Lahoz & De Lannoy, 2014) and therefore likely contributes substantially to real uncertainty in forecasts of aerosol and pollutant transport. While not discussed here, soil moisture will also have a large influence on the amount of dust lofted from the surface in desert regions (Fécan et al., 1998). This study indicates that more frequent and improved measurements of soil moisture and ocean/land surface properties are needed to reduce the uncertainty in the prediction of sea breeze dynamics and aerosol redistribution.

These results regarding tracer concentrations as a proxy for aerosol concentrations apply to our idealized case of a sea breeze without moist convection. Of course, clouds will also have an impact on local air quality conditions here. A follow-up study will address this more complicated scenario.

## Appendix A

Here we describe the sea breeze identification algorithm. First, we create a “strong” sea breeze mask using the surface potential temperature and cross-coast wind speed averaged in the along-coast direction every 30 min. The criteria are that the sea breeze does not exist over the ocean or before sunrise, that the potential temperature gradient is less than  $0.1 \text{ K m}^{-1}$ , that the wind is inland-directed, and that the wind speed gradient is negative and greater in magnitude than a quarter of the maximum negative wind speed gradient found throughout the entire simulation. In many simulations, these criteria alone are sufficient to identify a good sea breeze mask. However, in complex cases, these criteria are insufficient.

Figure A1 demonstrates the procedure for a particularly challenging case. Figure A1a shows the cross-coast wind speed. The sea breeze is clearly visible and exists from the coastline to the edge of the domain. Strong gradients in the wind speed also exist ahead of the front due to gravity wave activity. The strong mask is shown in Figure A1b. The strong mask identifies many points that do not correspond to the sea breeze, it is not continuous in time and space, and it does not start at the coast line.

Thus, as a second step, we also create a “weak” sea breeze mask. It uses the same criteria as the strong mask, except that points with a wind speed gradient greater in magnitude than one twentieth (rather than one quarter) of the maximum negative wind speed gradient are included and the inland-directed wind requirement is removed. This weak mask is shown in Figure A1c. It contains far too many points far from the sea breeze but has the advantage of fully including the sea breeze.

Using the weak sea breeze mask, we first pad the region and fill small holes (Figure A1d). Then MATLAB’s “bwconncomp” function is used to identify connected groups of points. Points are considered connected

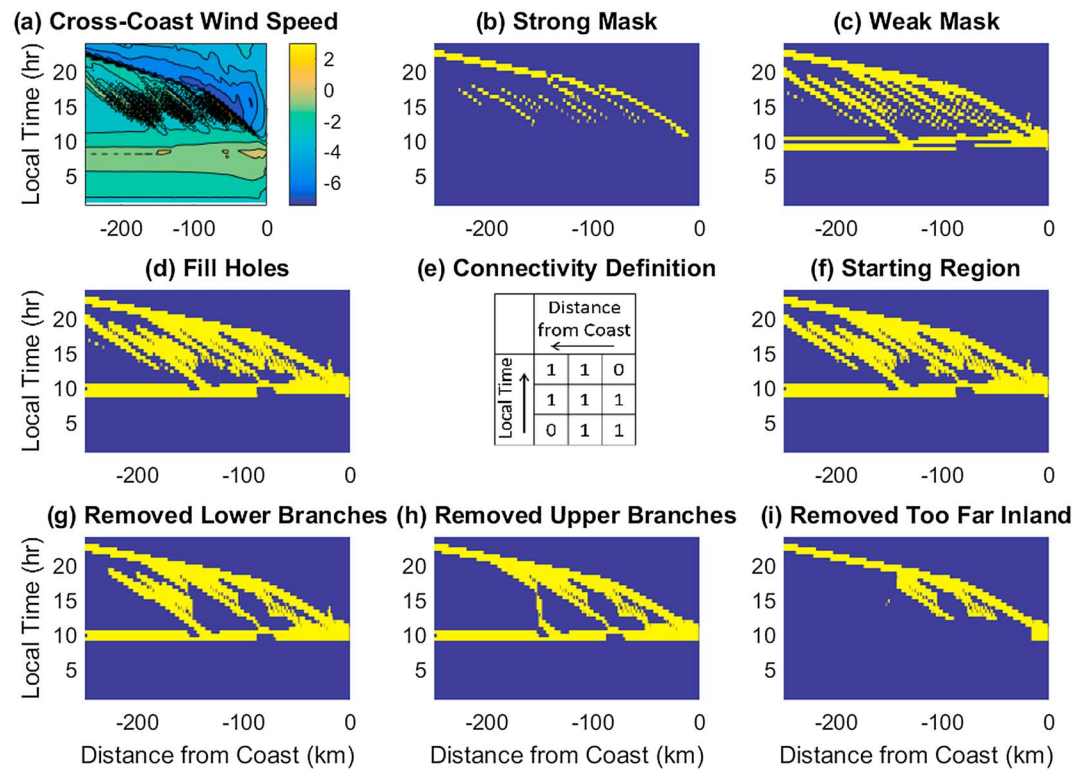


**Figure A1.** A demonstration of part of the sea breeze identification algorithm for one sea breeze simulation. (a) Cross-coast wind speed as a function of time and distance inland from the coast. (b–d and f–i) Potential sea breeze locations in yellow after each step of the algorithm. Details about each step are found in Appendix A. (e) Definition of connectivity.

according to Figure A1e where grid boxes labeled 1 are considered neighbors of the central box. The connected region that corresponds to the sea breeze is identified as the one containing the greatest number of points from the strong sea breeze mask (Figure A1f; the “starting region”).

For the case in Figure A1, the starting region still contains far too many points that are not near to the sea breeze. These points appear as branches from the “true” sea breeze location. These branches are systematically removed (Figures A1g and A1h). Finally, the remaining points in the starting region that extend further inland than the maximum extent of the sea breeze as determined from the strong sea breeze mask at each output time are also eliminated (Figure A1i).

From this final set of points, the sea breeze location is determined. Starting at the first output time with an identified sea breeze, its location is identified as the point with the minimum (most negative) value of the second spatial derivative of the wind speed. Restrictions on the propagation speed are applied for subsequent times. This procedure for identifying the sea breeze location at each time is repeated until the end of the sea breeze is reached.

**References**

Anderson, J. C., Wang, J., Zeng, J., Leptoukh, G., Petrenko, M., Ichoku, C., & Hu, C. (2013). Long-term statistical assessment of Aqua-MODIS aerosol optical depth over coastal regions: Bias characteristics and uncertainty sources. *Tellus Series B: Chemical and Physical Meteorology*, 65(1), 20,805. <https://doi.org/10.3402/tellusb.v65i0.20805>

Arritt, R. W. (1993). Effects of the large-scale flow on characteristic features of the sea breeze. *Journal of Applied Meteorology*, 32(1), 116–125. [https://doi.org/10.1175/1520-0450\(1993\)032<0116:EOTLSF>2.0.CO;2](https://doi.org/10.1175/1520-0450(1993)032<0116:EOTLSF>2.0.CO;2)

Azorin-Molina, C., Chen, D., Tijm, S., & Baldi, M. (2011). A multi-year study of sea breezes in a Mediterranean coastal site: Alicante (Spain). *International Journal of Climatology*, 31(3), 468–486. <https://doi.org/10.1002/joc.2064>

Baker, R. D., Lynn, B. H., Boone, A., Tao, W. K., & Simpson, J. (2001). The influence of soil moisture, coastline curvature, and land-breeze circulations on sea-breeze-initiated precipitation. *Journal of Hydrometeorology*, 2(2), 193–211. [https://doi.org/10.1175/1525-7541\(2001\)002<0193:TIOSMC>2.0.CO;2](https://doi.org/10.1175/1525-7541(2001)002<0193:TIOSMC>2.0.CO;2)

Chiba, O., Kobayashi, F., Naito, G., & Sassa, K. (1999). Helicopter observations of the sea breeze over a coastal area. *Journal of Applied Meteorology*, 38(4), 481–492. [https://doi.org/10.1175/1520-0450\(1999\)038<0481:HOOTSB>2.0.CO;2](https://doi.org/10.1175/1520-0450(1999)038<0481:HOOTSB>2.0.CO;2)

**Acknowledgments**

A. L. Igel and S. C. van den Heever have been supported by ONR grant N00014-16-1-2040. This grant is an Office of Naval Research funded by the Multi-disciplinary University Research Initiative (MURI) that is being led by PI Steven Miller. We thank the MURI team, in particular Sonia Kreidenweis and Samuel Atwood, for their input on this study. J. S. Johnson was supported by the UK-China Research & Innovation Partnership Fund through the Met Office Climate Science for Service Partnership (CSSP) China as part of the Newton Fund and by the Natural Environment Research Council ACIDPRUF (grant NE/I020059/1) and GASSP (grant NE/J024252/1) projects. The simulations were performed at the Navy Department of Defense Supercomputing Resource Center, and the output data are archived at Colorado State University. They are available upon request from A. L. Igel (aigel@ucdavis.edu) or S. C. van den Heever (Sue.vandenHeever@colostate.edu).

- Cotton, W. R., Pielke, R. A. Sr., Walko, R. L., Liston, G. E., Tremback, C. J., Jiang, H., ... McFadden, J. P. (2003). RAMS 2001: Current status and future directions. *Meteorology and Atmospheric Physics*, 82(1-4), 5–29. <https://doi.org/10.1007/s00703-001-0584-9>
- Crosman, E. T., & Horel, J. D. (2010). Sea and lake breezes: A review of numerical studies. *Boundary-Layer Meteorology*, 137(1), 1–29. <https://doi.org/10.1007/s10546-010-9517-9>
- Derimian, Y., Choël, M., Rudich, Y., Deboudt, K., Dubovik, O., Laskin, A., ... Karnieli, A. (2017). Effect of sea breeze circulation on aerosol mixing state and radiative properties in a desert setting. *Atmospheric Chemistry and Physics*, 17(18), 11,331–11,353. <https://doi.org/10.5194/acp-17-11331-2017>
- Drobinski, P., Rotunno, R., & Dubos, T. (2011). Linear theory of the sea breeze in a thermal wind. *Quarterly Journal of the Royal Meteorological Society*, 137(659), 1602–1609. <https://doi.org/10.1002/qj.847>
- Fécan, F., Marticorena, B., & Bergametti, G. (1998). Parametrization of the increase of the aeolian erosion threshold wind friction velocity due to soil moisture for arid and semi-arid areas. *Annales Geophysicae*, 17(1), 149–157. <https://doi.org/10.1007/s00585-999-0149-7>
- Finkele, K. (1998). Inland and offshore propagation speeds of a sea breeze from simulations and measurements. *Boundary-Layer Meteorology*, 87(2), 307–329. <https://doi.org/10.1023/a:1001083913327>
- Freitas, E. D., Rozoff, C. M., Cotton, W. R., & Silva Dias, P. L. (2006). Interactions of an urban heat island and sea-breeze circulations during winter over the metropolitan area of São Paulo, Brazil. *Boundary-Layer Meteorology*, 122(1), 43–65. <https://doi.org/10.1007/s10546-006-9091-3>
- Grant, L. D., & van den Heever, S. C. (2014). Aerosol-cloud-land surface interactions within tropical sea breeze convection. *Journal of Geophysical Research: Atmospheres*, 119, 8340–8361. <https://doi.org/10.1002/2014JD021912>
- Harrington, J. Y. (1997). The effects of radiative and microphysical processes on simulation of warm and transition season Arctic stratus. (PhD thesis), (289 pp.). Colorado State University.
- Johnson, J. S., Cui, Z., Lee, L. A., Gosling, J. P., Blyth, A. M., & Carslaw, K. S. (2015). Evaluating uncertainty in convective cloudmicrophysics using statistical emulation. *Journal of Advances in Modeling Earth Systems*, 7, 162–187. <https://doi.org/10.1002/2014MS000383>
- Lahoz, W. A., & De Lannoy, G. J. M. (2014). Closing the gaps in our knowledge of the hydrological cycle over land: Conceptual problems. *Surveys in Geophysics*, 35(3), 623–660. <https://doi.org/10.1007/s10712-013-9221-7>
- Lawrence, M. G., & Lelieveld, J. (2010). Atmospheric pollutant outflow from southern Asia: A review. *Atmospheric Chemistry and Physics*, 10(22), 11,017–11,096. <https://doi.org/10.5194/acp-10-11017-2010>
- Lee, L. A., Carslaw, K. S., Pringle, K. J., Mann, G. W., & Spracklen, D. V. (2011). Emulation of a complex global aerosol model to quantify sensitivity to uncertain parameters. *Atmospheric Chemistry and Physics*, 11(23), 12,253–12,273. <https://doi.org/10.5194/acp-11-12253-2011>
- Lee, L. A., Pringle, K. J., Reddington, C. L., Mann, G. W., Stier, P., Spracklen, D. V., ... Carslaw, K. S. (2013). The magnitude and causes of uncertainty in global model simulations of cloud condensation nuclei. *Atmospheric Chemistry and Physics*, 13(17), 8879–8914. <https://doi.org/10.5194/acp-13-8879-2013>
- Lombardo, K., Sinsky, E., Jia, Y., Whitney, M. M., & Edson, J. (2016). Sensitivity of simulated sea breezes to initial conditions in complex coastal regions. *Monthly Weather Review*, 144(4), 1299–1320. <https://doi.org/10.1175/mwr-d-15-0306.1>
- Loughner, C. P., Tzortziou, M., Follette-Cook, M., Pickering, K. E., Goldberg, D., Satam, C., ... Dickerson, R. R. (2014). Impact of bay-breeze circulations on surface air quality and boundary layer export. *Journal of Applied Meteorology and Climatology*, 53(7), 1697–1713. <https://doi.org/10.1175/jamc-d-13-0323.1>
- Lu, R., & Turco, R. P. (1994). Air pollutant transport in a coastal environment. 1. 2-dimensional simulations of sea-breeze and mountain effects. *Journal of the Atmospheric Sciences*, 51(15), 2285–2308. [https://doi.org/10.1175/1520-0469\(1994\)051<2285:APTIAC>2.0.CO;2](https://doi.org/10.1175/1520-0469(1994)051<2285:APTIAC>2.0.CO;2)
- Lyons, W. A., Pielke, R. A., Tremback, C. J., Walko, R. L., & Moon, D. A. (1995). Modeling impacts of mesoscale vertical motions upon coastal zone air pollution dispersion. *Atmospheric Environment*, 29(2), 283–301.
- Mazzuca, G. M., Pickering, K. E., Clark, R. D., Loughner, C. P., Fried, A., Stein Zweers, D. C., ... Dickerson, R. R. (2017). Use of tetheredsonde and aircraft profiles to study the impact of mesoscale and microscale meteorology on air quality. *Atmospheric Environment*, 149, 55–69. <https://doi.org/10.1016/j.atmosenv.2016.10.025>
- Miao, Y. C., Hu, X. M., Liu, S. H., Qian, T. T., Xue, M., Zheng, Y. J., & Wang, S. (2015). Seasonal variation of local atmospheric circulations and boundary layer structure in the Beijing-Tianjin-Hebei region and implications for air quality. *Journal of Advances in Modeling Earth Systems*, 7(4), 1602–1626. <https://doi.org/10.1002/2015JC000522>
- Miller, S. T. K., Keim, B. D., Talbot, R. W., & Mao, H. (2003). Sea breeze: Structure, forecasting, and impacts. *Reviews of Geophysics*, 41(3), 1011. <https://doi.org/10.1029/2003RG000124>
- Monteiro, A., Gama, C., Candido, M., Ribeiro, I., Carvalho, D., & Lopes, M. (2016). Investigating ozone high levels and the role of sea breeze on its transport. *Atmospheric Pollution Research*, 7(2), 339–347. <https://doi.org/10.1016/j.apr.2015.10.013>
- Moorthy, K. K., Murthy, B. V. K., & Nair, P. R. (1993). Sea-breeze front effects on boundary-layer aerosols at a tropical coastal station. *Journal of Applied Meteorology*, 32, 1196–1205.
- O'Hagan, A. (2006). Bayesian analysis of computer code outputs: A tutorial. *Reliability Engineering & System Safety*, 91(10–11), 1290–1300. <https://doi.org/10.1016/j.res.2005.11.025>
- Papanastasiou, D. K., & Melas, D. (2009). Climatology and impact on air quality of sea breeze in an urban coastal environment. *International Journal of Climatology*, 29(2), 305–315. <https://doi.org/10.1002/joc.1707>
- Physick, W. L., & Smith, R. K. (1985). Observations and dynamics of sea-breezes in northern Australia. *Australian Meteorological Magazine*, 33(2), 51–63.
- Pujol, G., looss, B., & Janon, A. (2013). Sensitivity: Sensitivity analysis, R package version 1.7.
- R Core Team (2015). *R: A language and environment for statistical computing*. Vienna, Austria: R Foundation for Statistical Computing.
- Reynolds, R. W., Smith, T. M., Liu, C., Chelton, D. B., Casey, K. S., & Schlax, M. G. (2007). Daily high-resolution-blended analyses for sea surface temperature. *Journal of Climate*, 20(22), 5473–5496. <https://doi.org/10.1175/2007jcli1824.1>
- Rotunno, R. (1983). On the linear theory of the land and sea breeze. *Journal of the Atmospheric Sciences*, 40(8), 1999–2009. [https://doi.org/10.1175/1520-0469\(1983\)040<1999:OTLTOT>2.0.CO;2](https://doi.org/10.1175/1520-0469(1983)040<1999:OTLTOT>2.0.CO;2)
- Roustant, O., Ginsbourger, D., & Deville, Y. (2012). DiceKriging, DiceOptim: Two R packages for the analysis of computer experiments by kriging-based metamodeling and optimization. *Journal of Statistical Software*, 51(1), 1–55.
- Russo, A., Gouveia, C., Levy, I., Dayan, U., Jerez, S., Mendes, M., & Trigo, R. (2016). Coastal recirculation potential affecting air pollutants in Portugal: The role of circulation weather types. *Atmospheric Environment*, 135, 9–19. <https://doi.org/10.1016/j.atmosenv.2016.03.039>
- Saleeby, S. M., & van den Heever, S. C. (2013). Developments in the CSU-RAMS aerosol model: Emissions, nucleation, regeneration, deposition, and radiation. *Journal of Applied Meteorology and Climatology*, 52(12), 2601–2622. <https://doi.org/10.1175/jamc-d-12-0312.1>
- Saltelli, A., Chan, K., & Scott, E. M. (2000). *Sensitivity Analysis*. New York: John Wiley.
- Saltelli, A., Tarantola, S., & Chan, K. P. S. (1999). A quantitative model-independent method for global sensitivity analysis of model output. *Technometrics*, 41(1), 39–56. <https://doi.org/10.2307/1270993>

- Sha, W. M., Kawamura, T., & Ueda, H. (1991). A numerical study on sea land breezes as a gravity current—Kelvin-Helmholtz billows and inland penetration of the sea-breeze front. *Journal of the Atmospheric Sciences*, *48*(14), 1649–1665. [https://doi.org/10.1175/1520-0469\(1991\)048<1649:ANSOSB>2.0.CO;2](https://doi.org/10.1175/1520-0469(1991)048<1649:ANSOSB>2.0.CO;2)
- Simpson, J. E. (1994). *Sea breeze and local winds* (234 pp.). UK: Cambridge University Press.
- Simpson, J. E., & Britter, R. E. (1980). A laboratory model of an atmospheric mesofront. *Quarterly Journal of the Royal Meteorological Society*, *106*(449), 485–500.
- Simpson, J. E., Mansfield, D. A., & Milford, J. R. (1977). Inland penetration of sea-breeze fronts. *Quarterly Journal of the Royal Meteorological Society*, *103*(435), 47–76. <https://doi.org/10.1002/qj.49710343504>
- Verma, S., Boucher, O., Venkataraman, C., Reddy, M. S., Müller, D., Chazette, P., & Crouzille, B. (2006). Aerosol lofting from sea breeze during the Indian Ocean Experiment. *Journal of Geophysical Research*, *111*, 07208. <https://doi.org/10.1029/2005JD005953>
- Walko, R. L., Band, L. E., Baron, J., Kittel, T. G. F., Lammers, R., Lee, T. J., ... Vidale, P. L. (2000). Coupled atmosphere, biophysics and hydrology models for environmental modeling. *Journal of Applied Meteorology*, *39*(6), 931–944. [https://doi.org/10.1175/1520-0450\(2000\)039<0931:CABHMF>2.0.CO;2](https://doi.org/10.1175/1520-0450(2000)039<0931:CABHMF>2.0.CO;2)
- Wang, C. C., & Kirshbaum, D. J. (2017). Idealized simulations of sea breezes over mountainous islands. *Quarterly Journal of the Royal Meteorological Society*, *143*(704), 1657–1669. <https://doi.org/10.1002/qj.3037>
- Wang, J., Ge, C., Yang, Z., Hyer, E. J., Reid, J. S., Chew, B.-N., ... Zhang, M. (2013). Mesoscale modeling of smoke transport over the Southeast Asian Maritime Continent: Interplay of sea breeze, trade wind, typhoon, and topography. *Atmospheric Research*, *122*, 486–503. <https://doi.org/10.1016/j.atmosres.2012.05.009>
- Yan, H., & Anthes, R. A. (1987). The effect of latitude on the sea breeze. *Monthly Weather Review*, *115*, 936–956. [https://doi.org/10.1175/1520-0493\(1987\)115<0936:TEOLOT>2.0.CO;2](https://doi.org/10.1175/1520-0493(1987)115<0936:TEOLOT>2.0.CO;2)